TNO Defence Research





Phone +31 70 326 42 21

TNO-report FEL-93-A039

copy nr.

title

An overview of the TNO contribution to VAST 92

(1)


[illegible] contains color plates: All DTIC reproductions will be in black and white.







TDCK RAPPORTENCENTRALE
Frederikkazerne, gebouw 140
v/d Burchlaan 31 MPC 16A
TEL. : 070-3166394/6395
FAX. : (31) 070-3166202
Postbus 90701
2509 LS Den Haag

# DISCLAIMER NOTICE


THIS DOCUMENT IS BEST QUALITY AVAILABLE. THE COPY FURNISHED TO DTIC CONTAINED A SIGNIFICANT NUMBER OF COLOR PAGES WHICH DO NOT REPRODUCE LEGIBLY ON BLACK AND WHITE MICROFICHE.

TNO Physics Laboratory

Oude Waalsdorperweg 63
2597 AK The Hague
P.O. Box 96864
2509 JG The Hague
The Netherlands

Fax +31 70 328 09 61
Phone +31 70 326 42 21



# TNO Defence Research

(1)

TNO-report FEL-93-A039

copy nr. 1

title

## An overview of the TNO contribution to VAST 92

author(s):

G.J. Kunz

M.M. Moerman



date:

August 1993

classification

classified by : W. Pelt

classification date : September 2, 1993

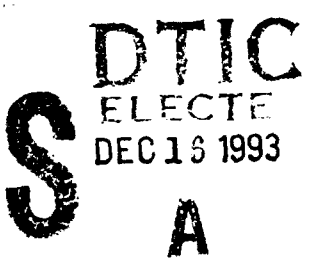

title : ongerubriceerd

abstract : ongerubriceerd

report text : ongerubriceerd

appendix A : ongerubriceerd

This document has been approved for public release and sale; its distribution is unlimited

no. of copies : 38

no. of pages : 42 (including appendix, excluding RDP and distribution list)

no of appendices : 1

*Original contains color plates: All DTIC reproductions will be in black and white*

All information which is classified according to Dutch regulations shall be treated by the recipient in the same way as classified information of corresponding value in his own country. No part of this information will be disclosed to any party.

The classification designation ongerubriceerd is equivalent to unclassified.

report no. : FEL-93-A039

title : An overview of the TNO contribution to VAST 92

author(s) : G.J. Kunz and M.M. Moerman

institute : TNO Physics and Electronics Laboratory

date : August 1993

NDRO no. : A90K703

no. in pow '93 : 715.1

Research supervised by:

Research carried out by:

## ABSTRACT (ONGERUBRICEERD)

The 'Vertical Atmospheric Structure Trial' (VAST92) took place from September 28 to October 16, 1992 at the Wehr Technische Dienststelle (WTD 52), Oberjettenberg, Germany, in the framework of NATO working group AC/243 (Panel 4/RSG.8) on atmospheric propagation effects on electro-optical systems. The experiment was designed to quantify the influence of the atmospheric vertical structure variations on infrared propagation and imaging and on lidar means of remotely sensing the variations. The TNO-Physics and Electronics Laboratory participated with a lidar system, meteo and aerosol equipment. The lidar was stationed in the valley. An altimeter and meteo-equipment were mounted on the cable car. Aerosol spectrometers and meteorological equipment were used, including a sonic anemometer and a fast hygrometer to measure turbulence on the mountain. A large part of the data from these instruments is of crucial importance for the evaluation and interpretation of the data obtained by the other participants.

In this report, we present an overview of the TNO instrumentation and experiments. A number of data sets have been processed to demonstrate the possibilities of the different instruments. Interpretation of the results is postponed to later reports. This report is also a guide-line for processing the TNO data in conjunction with data from other participants.

| | | |
|---|---|---|
| rapport no. | : | FEL-93-A039 |
| titel | : | Een overzicht van de TNO bijdrage aan VAST 92 |
| auteur(s) | : | Ir. G.J. Kunz en M.M. Moerman |
| instituut | : | Fysisch en Elektronisch Laboratorium TNO |
| datum | : | augustus 1993 |
| hdo-opdr.no. | : | A90K703 |
| no. in iwp '93 | : | 715.1 |
| Onderzoek uitgevoerd o.l.v. | : | |
| Onderzoek uitgevoerd door | : | |

SAMENVATTING (ONGERUBRICEERD)

De 'Vertical Atmospheric Structure Trial' (VAST92) werd gehouden van 28 september tot 16 oktober 1992 bij de Wehr Technische Dienststelle (WTD 52), Oberjettenberg, Duitsland in het kader van NATO werkgroep AC/243 (Panel 4/RSG.8) ('Atmospheric propagation effects on electro-optical systems'). Het doel van dit experiment was om na te gaan wat de invloed is van de vertikale atmosferische struktuurvariaties op propagatie in het infrarood o.a. voor afbeeldende systemen en op lidar inversiemethoden die deze variaties kunnen meten. TNO Fysisch en Elektronisch Laboratorium heeft een substantiële bijdrage geleverd met een lidar in het dal, met meteorologische sensoren en een hoogtemeter aan de gondel. Aerosol spectrometers en meteorologische sensoren werden gebruikt, inclusief een sonische anemometer en een snelle vochtigheids-meter om turbulentie te kunnen meten op de berg. Een groot deel van de gegevens, verkregen met deze instrumenten, is van cruciaal belang bij de evaluatie en de interpretatie van de gegevens die door de andere deelnemers zijn verzameld.

In dit rapport geven we een overzicht van de door TNO gebruikte instrumenten en van de TNO experimenten. Een aantal data sets zijn uitgewerkt om de mogelijkheden van de verschillende instrumenten te laten zien en om aan te geven op welke wijze de data kan worden uitgewerkt en gepresenteerd. Dit rapport dient tevens als leidraad bij het uitwerken van alle beschikbare gegevens zoals gemeten door TNO, tezamen met de data van de andere deelnemers.

CONTENTS

# 1 INTRODUCTION

The 'Vertical Atmospheric Structure Trial' (VAST92) was organized from September 28 to October 16, 1992 at the Wehr Technische Dienststelle (WTD 52), Oberjettenberg, Germany, in the framework of NATO working group AC/243 (Panel 4/RSG.8) on Atmospheric propagation effects on electro-optical systems. The experiment was designed to quantify the influence of the atmospheric vertical structure variations on infrared propagation and imaging, and on lidar means of remotely sensing the variations. Dr. L.R. Bissonnette of DREV, Canada, was chairman of the scientific committee, which further consisted of Dr. A. Kohnle of FfO, Germany, who was responsible for the local organization. The WTD 52 cable car facilities provide a unique capability for performing slant path measurements over an altitude range from about 650 m to about 1700 m. The *in situ* measured results form the 'ground truth' data-base for evaluation of algorithms used to retrieve the slant path transmission from remote sensors (lidar) and for the assessment of the atmospheric effects on IR-imagers. More background information on this experiment has been described by Bissonnette, 1992a.

The TNO Physics and Electronics Laboratory participated with a Mie lidar in the valley and with supporting instruments on the cable car (meteo sensors + data recorders). At the mountain station, TNO provided meteo equipment, aerosol probes, an ultra-sonic anemometer (20 Hz) and an IR hygrometer (20 Hz). In a later stage of the experiment, the ground temperature near Gredinger Haus was also measured for USAF participants.

Other participants participated with lidar systems, IR-imagers, meteo-, turbulence- and aerosol equipment, a dropsonde, transmissometers, a white-cell and others, as described in Bissonnette, 1992a.

The purposes of this report are to present an overview of the available TNO data-bases for other participants and to indicate the capabilities of our instruments. This is illustrated with some (partly) processed data.

Note: All the times mentioned in this report are local times, referred to the public Cesium clock of the 'Physikalisch Technischen Budesanstalt' in Braunschweig, Germany.

Impression of the weather

During the initial phase of the experiment, the weather was clear with sun shine during the day. In the second and third week, low-altitude clouds and cloud patches lasted for longer periods on and around the mountain, and in the valley. The estimated visibility in the clouds was about 25 m, as confirmed by human observation of recognizable objects from the cable car. The cloud layers dissolved sometimes within a few minutes when the sun rose over the mountain tops. Temperatures were all above the freezing point, except in the morning of 13 October. The horizontal wind speed along the mountain was in general less than a few meters per second. In the beginning of the third week, Gredinger Haus was in the sun, while the valley was covered with clouds.

A more extensive and day to day description of the weather situation has been given by Bissonnette, 1992b.

## 2 PARAMETERS, SENSORS AND LOCATIONS

The TNO instruments used during the experiment were either factory calibrated (e.g. IR-humidity sensor, pressure sensor and ultrasonic anemometer) or calibrated at the laboratory (e.g. temperature, relative humidity). Before and after the experiment, instrument comparisons were made (e.g. for temperature, pressure and wind). During the experiment, however, it appeared that the adjustments of the pre-amplifiers for the Rotronic and for the thermistor had changed during the final mechanical construction. The validated data (presented here) have been corrected for these effects.

An overview of the instruments used during the experiment, their locations, and the measured parameters is presented in Table 2.1.

Table 2.1: Overview of the instruments and the parameters measured by TNO in the valley, at the mountain top and on the cable car during VAST92.

| parameter | valley (see) Chapter 3 | cable car (see) Chapter 4 | mountain (see) Chapter 5 | Instrument |
|---|---|---|---|---|
| RH, TA | - | - | x | Hygrophyl |
| WS | - | x | x | Cup anemometer |
| WD | - | x | x | Wind vane |
| TA | - | x | - | Thermistor |
| LI | x | - | - | Lidar |
| WS, WD, TA | - | - | x | Sonic anemometer |
| RH, TA | - | - | x | IR hygrometer |
| PR, ALT | - | x | - | Pressure sensor 1 |
| PR | - | - | x | Pressure sensor 2 |
| RH, TA | - | x | - | Rotronic |
| RR | - | - | x | Rain Gauge |
| SI | - | - | x | Scatterometer |
| IR | - | - | x | Pyranometer |
| AE | - | - | x | Aerosol probes |
| GT | - | - | x | Thermistor |

Legend:

AE = aerosol particle size distribution
ALT = altimeter
GT = ground temperature near Gredinger Haus
IR = irradiation
LI = lidar
PR = atmospheric pressure
RH = relative humidity
RR = rain rate
SI = scattering intensity
TA = air temperature
WD = wind direction
WS = wind speed

One of the TNO data recorders on the cable car recorded also the outputs of the visibility meter and of the IR-scatterometer of DREV (both called 'visibility' meters in the rest of the report).

The instruments mentioned in Table 2.1 operated perfectly during the common measuring periods. The instruments on the mountain (meteo, ultra-sonic anemometer and IR-hygrometer) operated 24 hours per day. Detailed information, e.g. on the active periods and on the available data differentiated to location is presented in sections 3 to 5. This is illustrated with some typical examples. A general overview of all participants with their equipment has been presented by Bissonnette, 1992a,b.

# 3 INSTRUMENT IN THE VALLEY

The TNO SMAL-lidar was stationed in the valley to measure the vertical structure of the atmospheric scattering. This lidar system has been described by Kunz, 1991 and by Bissonnette, 1992b. Stimulated by Dr. Bissonnette's multi-field-of-view lidar, also some multiple scattering measurements were performed using an adjustable second receiver on top of the main lidar. Table 3.1 gives an overview of the active periods of the SMAL-lidar. Results will be presented in a forthcoming report.

Table 3.1: Active periods of the TNO SMAL-lidar, including the amount of data recorded.

| Date | Local Time | | | | | | | | | | | | | |
|---|---|---|---|---|---|---|---|---|---|---|---|---|---|---|
| October | 08 | 09 | 10 | 11 | 12 | 13 | 14 | 15 | 16 | 17 | 18 | 19 | 20 | Amount of data in by |
| 5 | | | ⌊ | ——— | ⌋ | | ⌊ | ——— | ⌋ | | | ⌊ | ⌋ | 7.410346 |
| 6 | | | ⌊ | ——— | ——— | ——— | ——— | ——— | ——— | | ⌊ | ——— | ⌋ | 12.332924 |
| 7 | | | ⌊ | ——— | ⌋ | | ⌊ | ——— | ⌋ | | ⌊ | ——— | ⌋ | 9.908076 |
| 8 | | | ⌊ | ——— | ⌋ | | | | | | ⌊ | ——— | ——— | 8.214856 |
| 9 | | | ⌊ | ⌋ | | | | | | | | | | 25.087205 |
| 10 | | ⌊ | ——— | ——— | ⌋ | | | ⌊ | ——— | ——— | ——— | ⌋ | | 21.145859 |
| 11 | | ⌊ | ——— | ——— | ——— | ⌋ | | ⌊ | ——— | ——— | ⌋ | | | 6.312870 |
| 12 | | | ⌊ | ——— | ⌋ | | | | | | | | | 7.103267 |
| 13 | | | ⌊ | ——— | ⌋ | | | | | | | | | 6.111559 |
| 14 | | | ⌊ | ——— | ——— | ⌋ | | | | | | | | 2.056995 |
| 15 | | ⌊ | ——— | ——— | ⌋ | | | | | | | | | 4.469186 |

# 4 INSTRUMENTS ON THE CABLE CAR

## 4.1 Introduction

An instrumented cable car (during the experiment also called 'gondola') was moved up and down along the mountain slope to characterize the vertical structure of the atmosphere. Sensors were used for temperature, relative humidity, visibility, aerosol size distribution, wind speed and wind direction. An overview of the TNO equipment on this cable car is presented in Table 4.1. In addition, TNO recorded the data of the DREV visibility meter and of the DREV IR-scatterometer.

Table 4.1: Sensors, provided by TNO, mounted on the cable car.

- clock
- thermistor
- relative humidity
- wind vane
- cup anemometer
- pressure (altimeter)

Figure 4.1 shows photographs of both sides of the instrumented cable car.

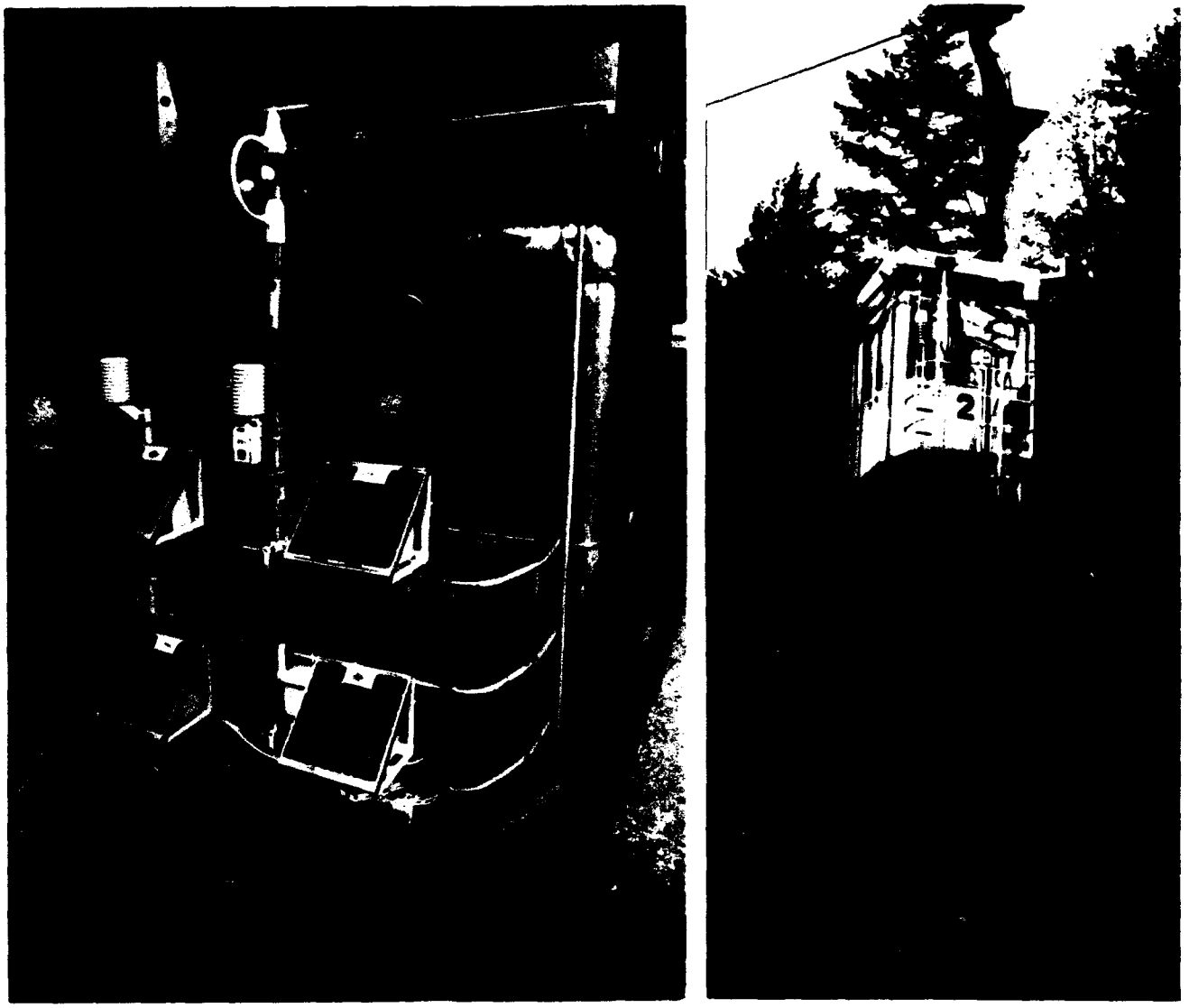

Figure 4.1: The instrumented cable car as seen from the mountain side (a) and from the valley side (b).

The TNO solar-cell-powered instruments with data recorders were mounted on the mountain side of the cable car. The thermistor and the Rotronic were both mounted in a white plastic radiation shield. The white mechanical protecting cap on the Rotronic was removed to increase the temporal response of this sensor. The pressure sensor was mounted in one of the solar-cell housings. The wind vane/cup anemometer was mounted on the ladder just above the roof of the cable car. We realize that the wind measurements at this place will often have been influenced by the cable car. The visibility meter (DREV), the IR-scatterometer (DREV), the aerosol equipment (FfO) and a second wind sensor (FfO) were mounted on the valley side of the cable car.

## 4.2 Calibration of the altimeter

The altitude of the cable car was determined with a pressure sensor which (recording) range has such been chosen (700 ... 1000 mBar) that it could handle both the normal atmospheric pressure variations and the pressure difference between the valley and the mountain station. Each 100 mBar interval was digitized with 8 bits which resulted in a height resolution of about 3 m. The actual conversion from pressure to altitude was calculated using time-series from the pressure sensor and from the length of the drawing-cable, as recorded during the test-run on 1 October. (The drawing-cable pulls the cable car up and down.) The relation between the length of the cable and the height of the cable car was provided by the proving ground. As a result, the conversion from pressure to height could be realized as outlined below in short.

The cross section of the mountain below the cable, the path of the cable car and the length of the drawing cable are presented in Figure 4.2. External influences on the shape of the cable profile, like temperature and load of the cable car, are not considered here. The height of the cable car has been expressed as a second order polynomial approximation in the drawing-cable length, as shown in the upper left of the figure. The influence of the cable-support, close to the mountain station, has been neglected.

Subsequently, the height of the cable car was expressed in the lengths of the drawing-cable (by eliminating the horizontal distance) and compared with the data from the pressure sensor. The results are shown in Figure 4.3. The triangles represent the height of the cable car as a function of the pressure and the small open circles represent the length of the drawing cable as a function of the pressure. The parameters for the linear approximation are shown in the figure.

A theoretical derivation of the relation between pressure and altitude for the Oberjettenberg situation is presented in Appendix A. The difference between the experimentally found gradient dZ/dP of 9.58 m/mBar and the theoretical value of 9.2 m/mBar might be caused by the non adiabatic lapse rate of the air temperature (Dr. J. Martin, private communications).

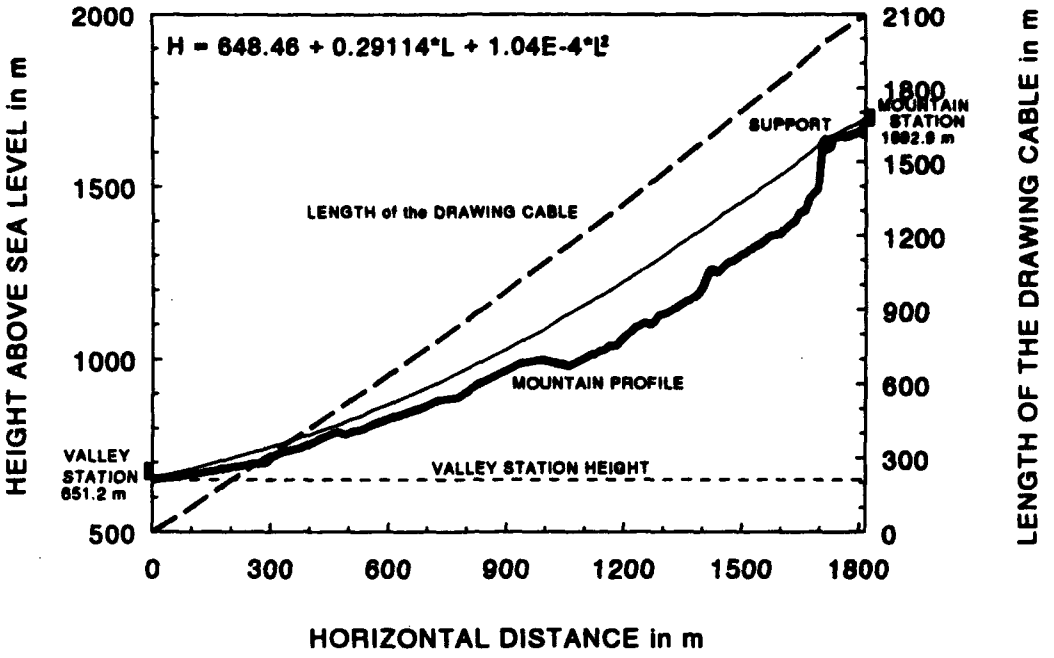


Figure 4.2: Cross section of the mountain (solid thick line) and profile of the support cable (solid thin line). The length of the drawing-cable versus the horizontal position is shown as a bold dashed line. A second order polynomial approximates the height of the cable car (H) in the length (L) of the drawing-cable.

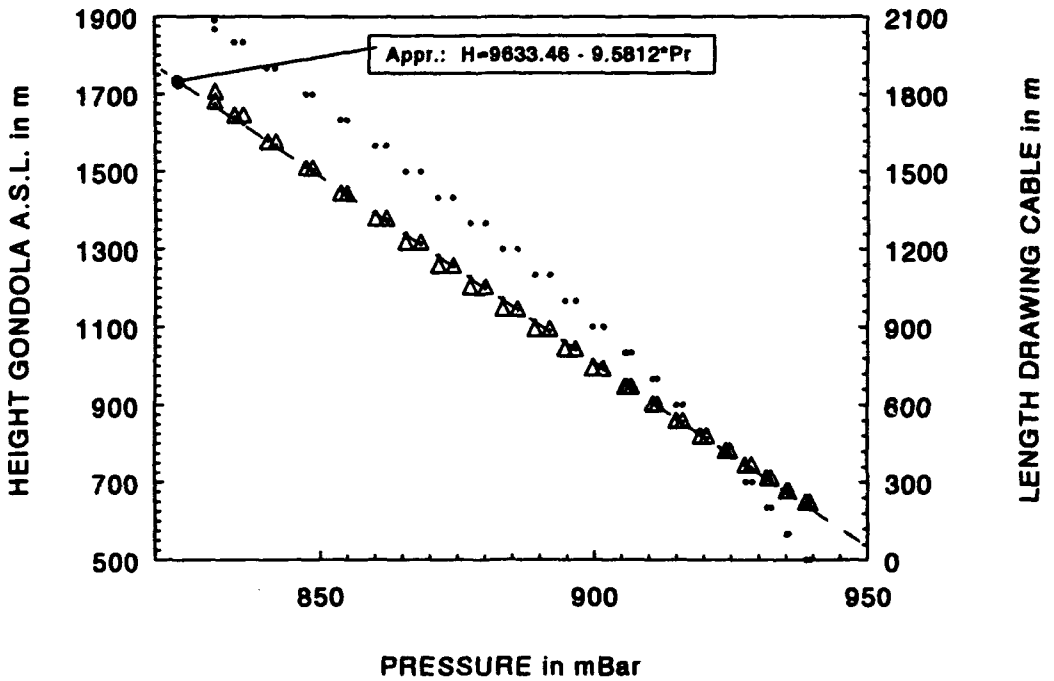


Figure 4.3: Height of the cable car (triangles) and the length of the drawing-cable (small open circles) as a function of the pressure. A linear approximation, expressing the height in the pressure, is shown as a dashed line and printed in the top of the figure.

## 4.3 Active periods

The TNO sensors and the data recorders were active during all formal cable car runs. Table 4.2 gives an overview of these active periods. Each horizontal line in the table represents one complete up and down trip. Runs with more than one up/down trip have been split (indicated by a series of dots). Separate runs on one day are identified in the first column by a letter (a,b,c,d). The last column shows the mode in which the cable car was transported: n(ormal) s(peed) (about 4 m/s), r(educed) s(peed) or in st(eps). Because the length of the drawing cable was about 2100 m, each ascent or descent at normal speed, including the start and stop procedure, lasted about 10 minutes.

Table 4.2: Overview of the runs of the instrumented cable car during VAST92. The bars indicate the duration of each run. The last column indicates the type of transportation (Normal Speed, Reduced Speed or STep wise).

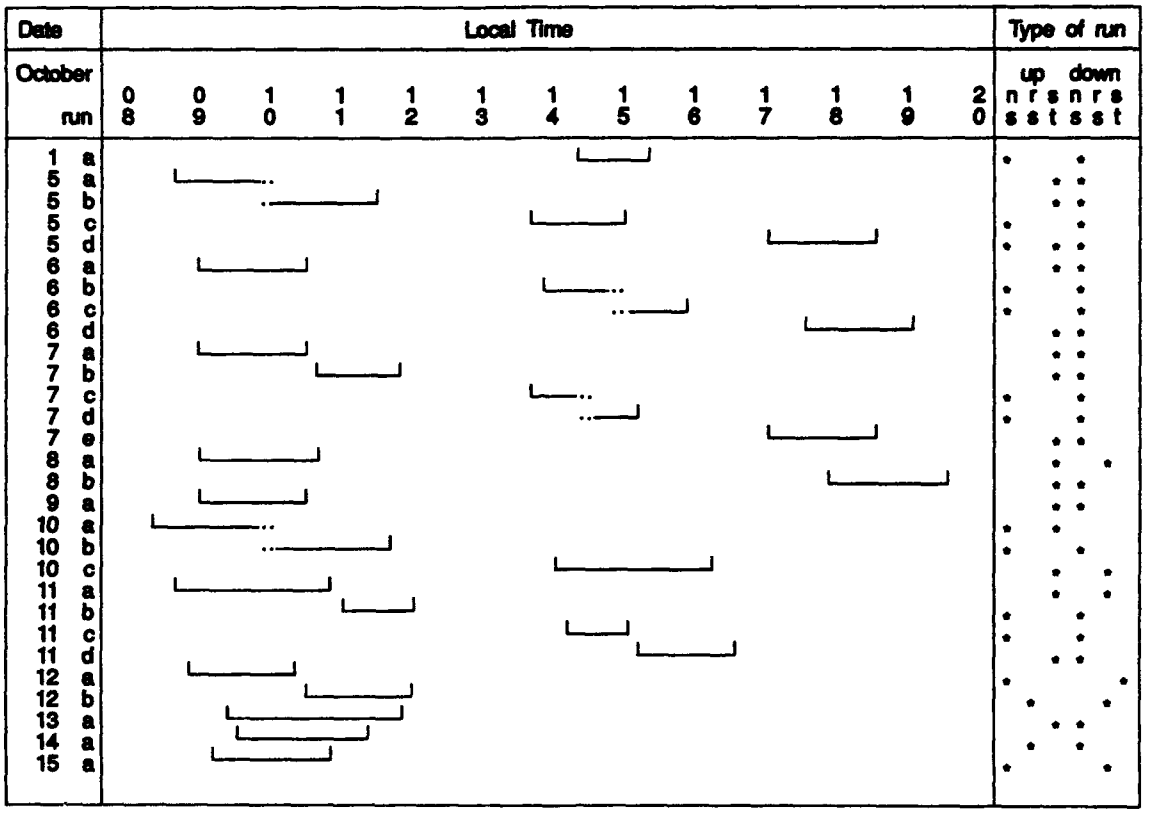

## 4.4 Some examples

The data of the sensors in the cable car can either be presented as a function of time or as a function of altitude. The final choice, of course, depends on the requirements of the user but one should keep in mind that the atmosphere may vary both in time and space in this orographic environment. As a result, the data obtained during the ascent and the descent may be different. Therefore, the results will both be plotted as a function of time and as a function of pressure (altitude) to illustrate the difference.

The selected data-set is from the cable car run on 9 October 1992, from 09:00 to 10:30 a.m., when slowly dissolving low lying clouds drifted in the valley. On the mountain, however, the sun was shining. The ascent of the cable car was in steps, stopping for about 5 minutes at fixed heights; the descend was at normal speed.

Figure 4.4 a..d shows the results as a function of time and Figure 4.5 a..d shows the same results as a function of altitude.

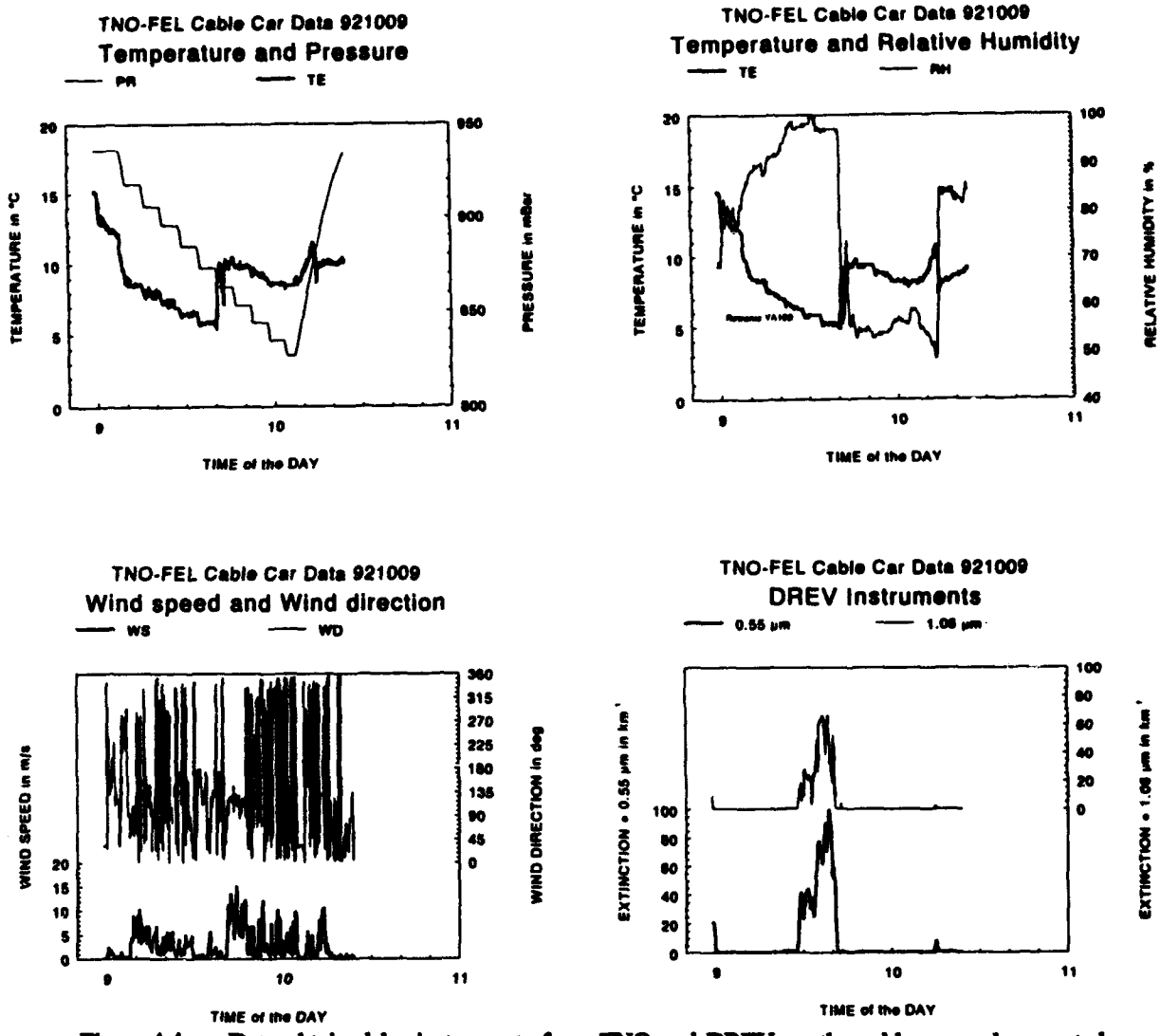


Figure 4.4: Data obtained by instruments from TNO and DREV on the cable car and presented as a function of time (9 October 1992). See also Figure 4.5 for a presentation as a function of altitude.

Figure 4.4a shows the step wise change in the pressure during the ascent and the smooth increase in pressure during the descent. The temperature was measured with the thermistor.

Figure 4.4b shows the temperature and relative humidity as a function of time, both measured with the Rotronic. The temperature decreased and the relative humidity increased while the cable car moved further into the cloud. At about 09:40 a.m., the cable car reached the top of the cloud resulting in a sudden drop in relative humidity and an increase in temperature (top of the cloud is also confirmed by the DREV 'visibility' meters).

Figure 4.4c shows the results of the wind-meter. The wind direction is difficult to determine because the wind speed was low.

Figure 4.4d shows the results from the DREV 'visibility' meters indicating the presence of the cloud layer during the ascent and the (almost) absence of this layer during the descent. This can be important during the interpretation of the lidar data.

The data shown in Figure 4.4 has also been plotted as a function of altitude, see Figure 4.5a..d.

The results of Figure 4.5 show that the vertical atmospheric variations are significant, both in time and in space. Furthermore, it becomes clear that the cloud layer had partly been dissolved during the descent as can be seen in the relative humidity and the extinction.

Note: The instrumented cable car was normally parked in a hall. Some minutes before the cable car departed, the instruments and the data-recorders were started. Therefore, the peak values in the beginning of the figures indicate the difference in climate between the atmosphere outside and in the hall.

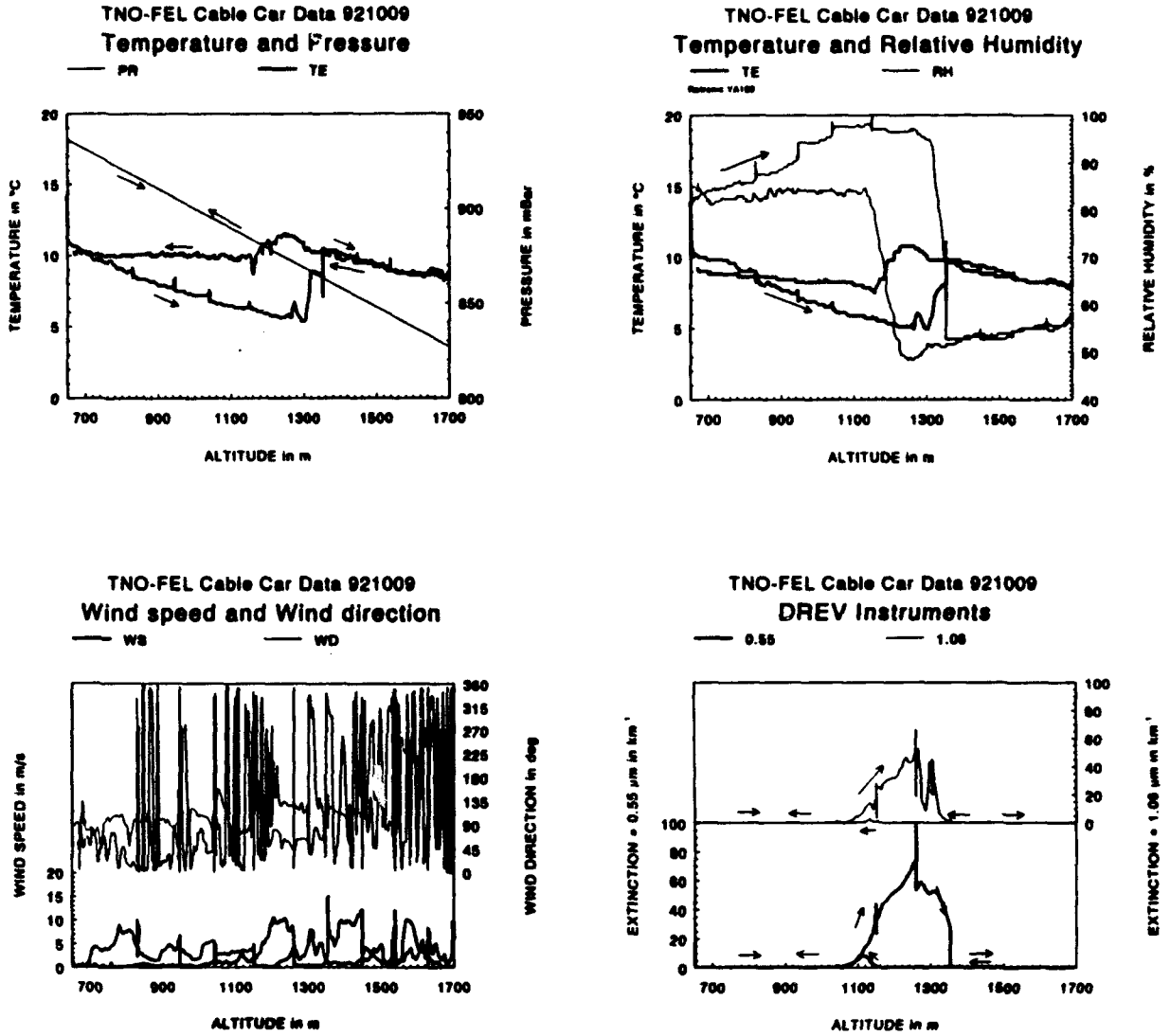


Figure 4.5: Data obtained by instruments from TNO and DREV on the cable car, presented as a function of altitude (9 October 1992). See also Figure 4.4 for a presentation as a function of time.

# 5 INSTRUMENTS ON THE MOUNTAIN

## 5.1 Introduction

On the mountain, at about 5 meters from Gredinger Haus, TNO measured temperature, pressure, wind speed and wind direction, relative humidity, aerosol particle size distribution, irradiation and precipitation. The location was one of the highest points within the area, providing an unobstructed view over the valley station in the northern direction close to a steep slope. In the other directions, the surface was sloping and covered with low green pine shrubs. A schematic overview of the locations of the TNO instruments is given in Figure 5.1.

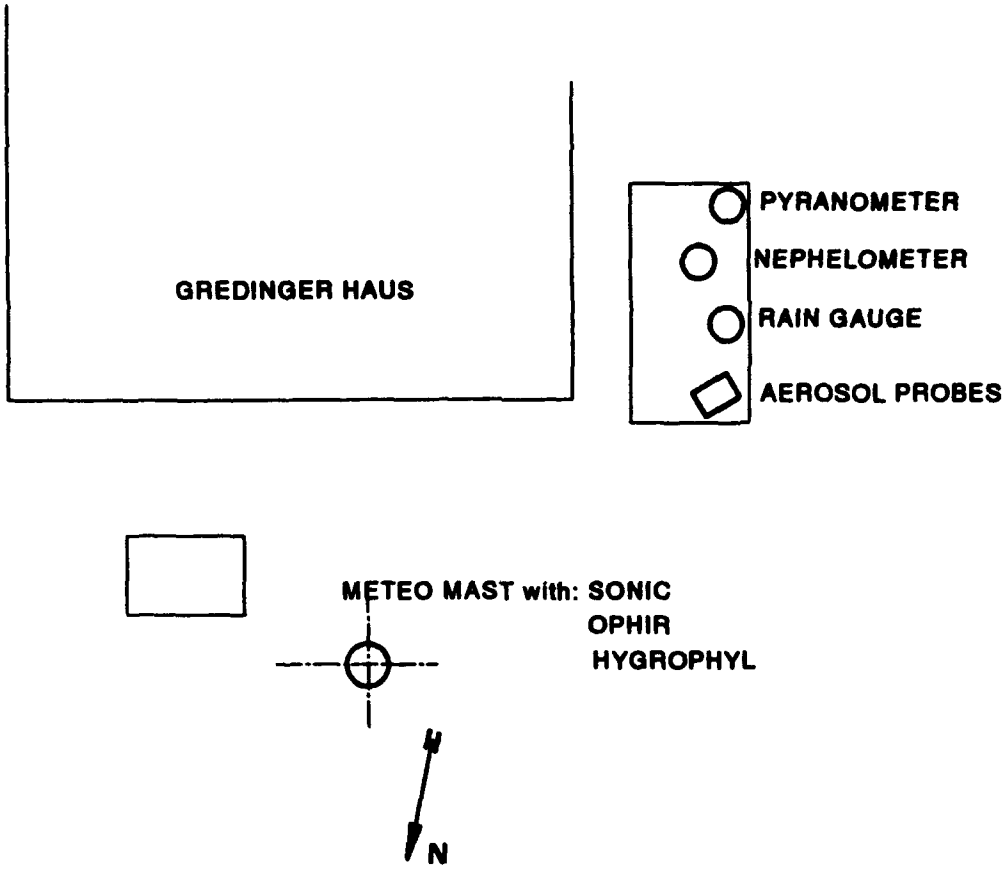


Figure 5.1: Locations of the TNO instruments around the mountain station.

The pyranometer, the nephelometer, the rain gauge and the aerosol probes were placed on a wooden platform (3x6 $m^2$), about 4 m from the southern wall of the house. The aerosol probes were placed at 75 and 95 cm above the platform. The inlets of were manually directed into the wind.

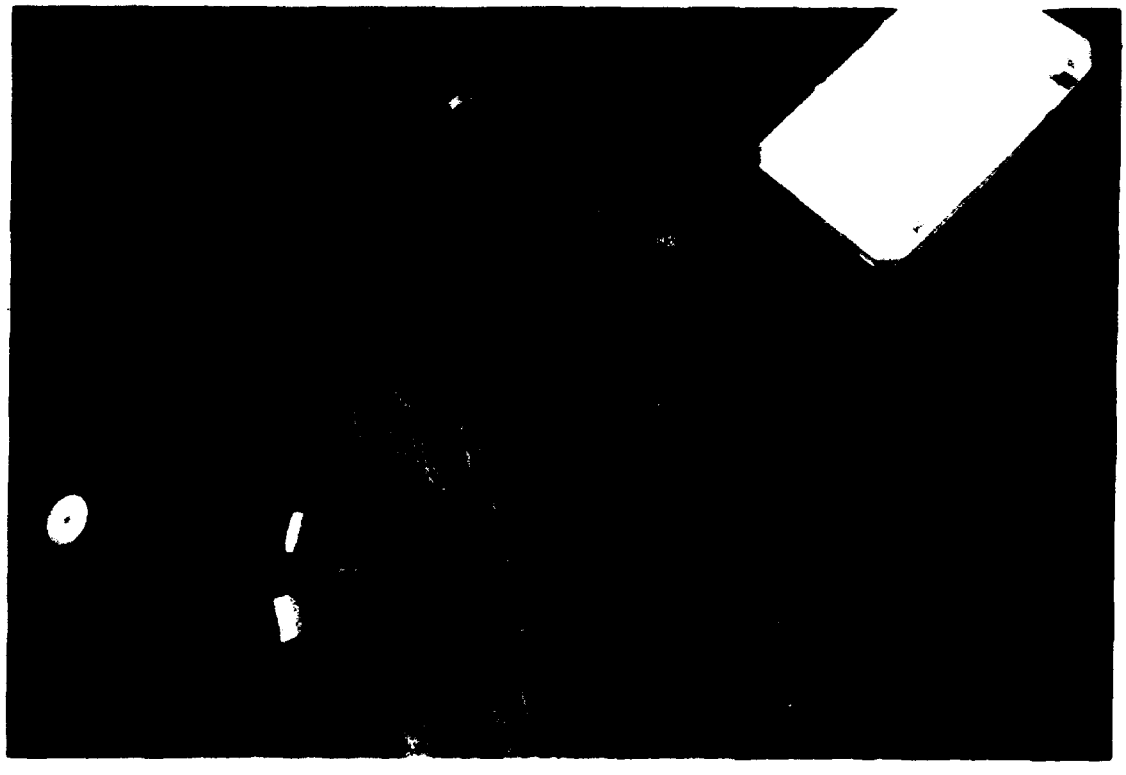

Figure 5.2: Overview of the TNO instruments on the wooden platform near Gredinger Haus. From left to right: pyranometer, nephelometer, Marcel Moerman near the rain gauge and the boxes with the aerosol probes.

The ultra-sonic anemometer, the IR hygrometer and the cup anemometer/wind vane were mounted on a 5 m high mast at about 6 m from the house, as close as possible to the ridge of the mountain, with a free aspect to the instruments in the valley. The (top of the) mast is shown in Figure 5.3.

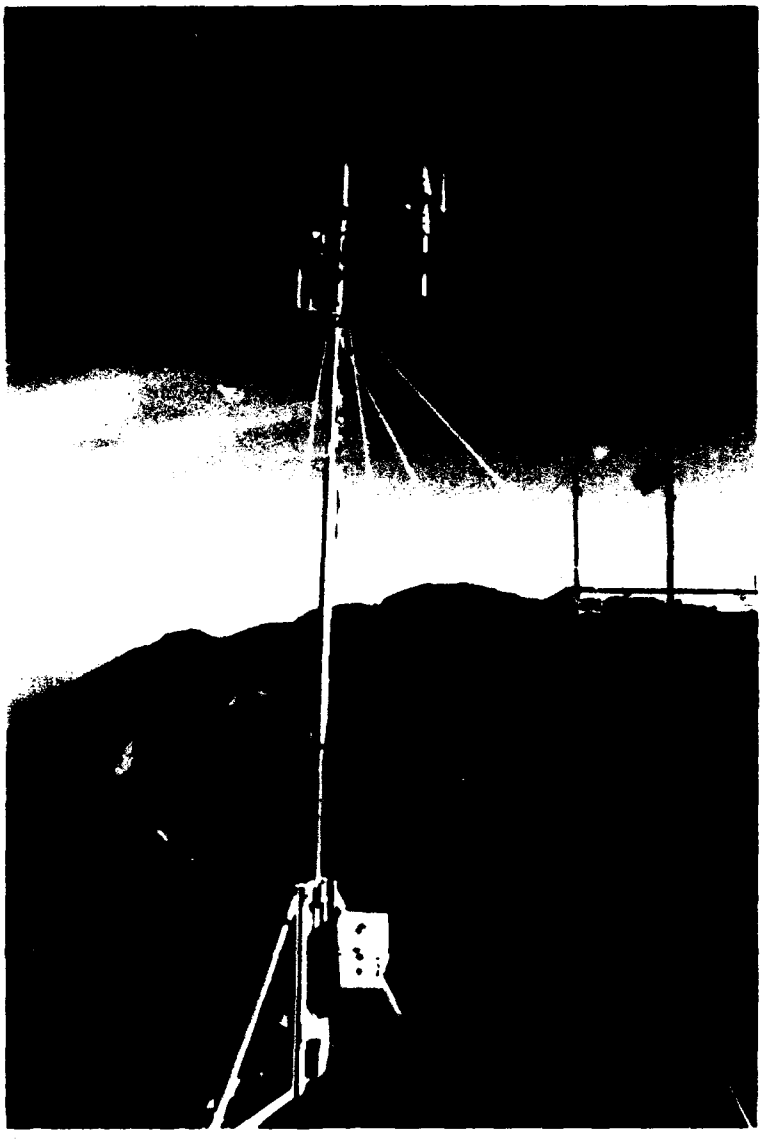

Figure 5.3: The TNO meteo mast near 'Gredinger Haus' with the ultra-sonic anemometer on top and below the IR-hygrometer on the left and the cup anemometer/wind vane on the right.

Both the location of the instruments on the wooden platform and the location of the mast were such that the sensors were in the prevailing wind direction.

About 1 m from the ground (not shown in Figure 5.3), an hygrophyl (wet and dry bulb) sensor was mounted on the mast.

In the next three sections, an overview will be presented of the available data sets as obtained with the TNO sensors on the mountain. Some examples of the data are shown. Each section represents a typical group of instruments:

- meteo, sampling rate 1 Hz, averaged over 5 minutes
  see section 5.2

- turbulent air flow and humidity, sampling rate 20 Hz
  see section 5.3

- aerosol counters, integrating time 5 minutes or less, depending on the weather conditions
  see section 5.4.

## 5.2 Meteo station; active periods and examples

The actual meteorological condition on the mountain was measured with the following instruments:

| | |
|---|---|
| wind vane | - Thies |
| cup anemometer | - Thies |
| dry and wet bulb | - hygrophil |
| pyranometer | - Kip en Zn, CM 6, 305..2800 nm |
| rain gauge | - TNO-FEL |
| nephelometer | - TNO-FEL |
| pressure sensor | - Honeywell |

The sensors were sampled each second; the 5-minutes averaged values and their standard deviations were stored. The meteo sensors have been operated unattended 24-hours per day, except for short periods which were required to copy the data to diskette. An overview of the available data sets is presented in Table 5.1. As an example, the data collected on 9 October with the slow meteo equipment are presented in Figure 5.4a..d.

Table 5.1: Overview of the active times of the TNO-meteo station near Gredinger Haus.

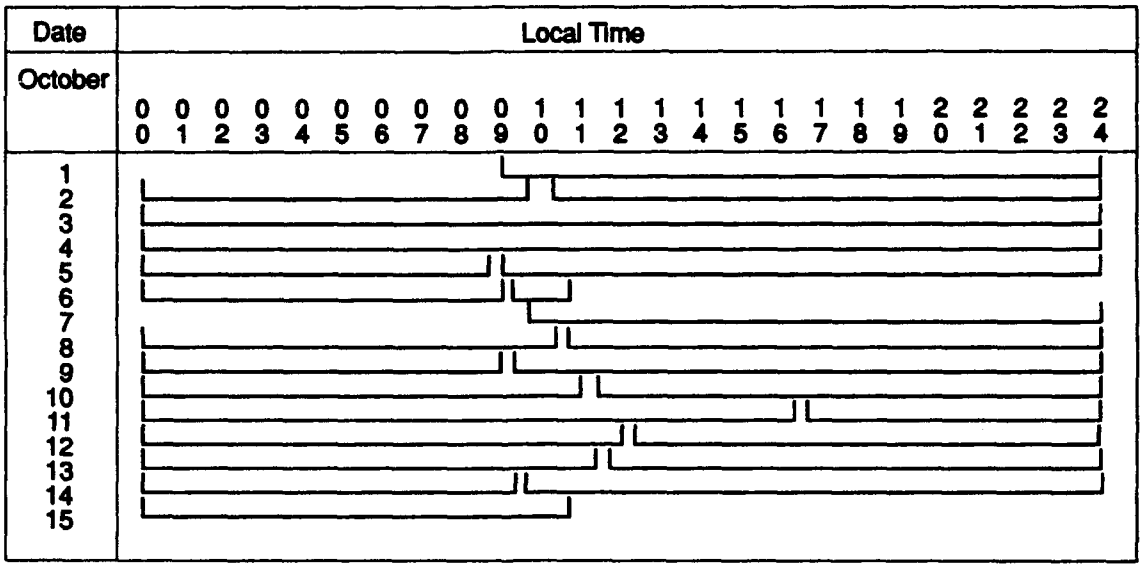


Notes:

1. the bars indicate the active periods
2. the gaps, which are generally shorter than 15 minutes, show the daily interrupts for storing and copying of the data
3. the gap on 6 October from 10:40 a.m. to 7 October 09:30 a.m., was partly caused by an unknown reason and partly by a power failure
4. an announced power failure occurred on 7 October at 05:00 p.m.

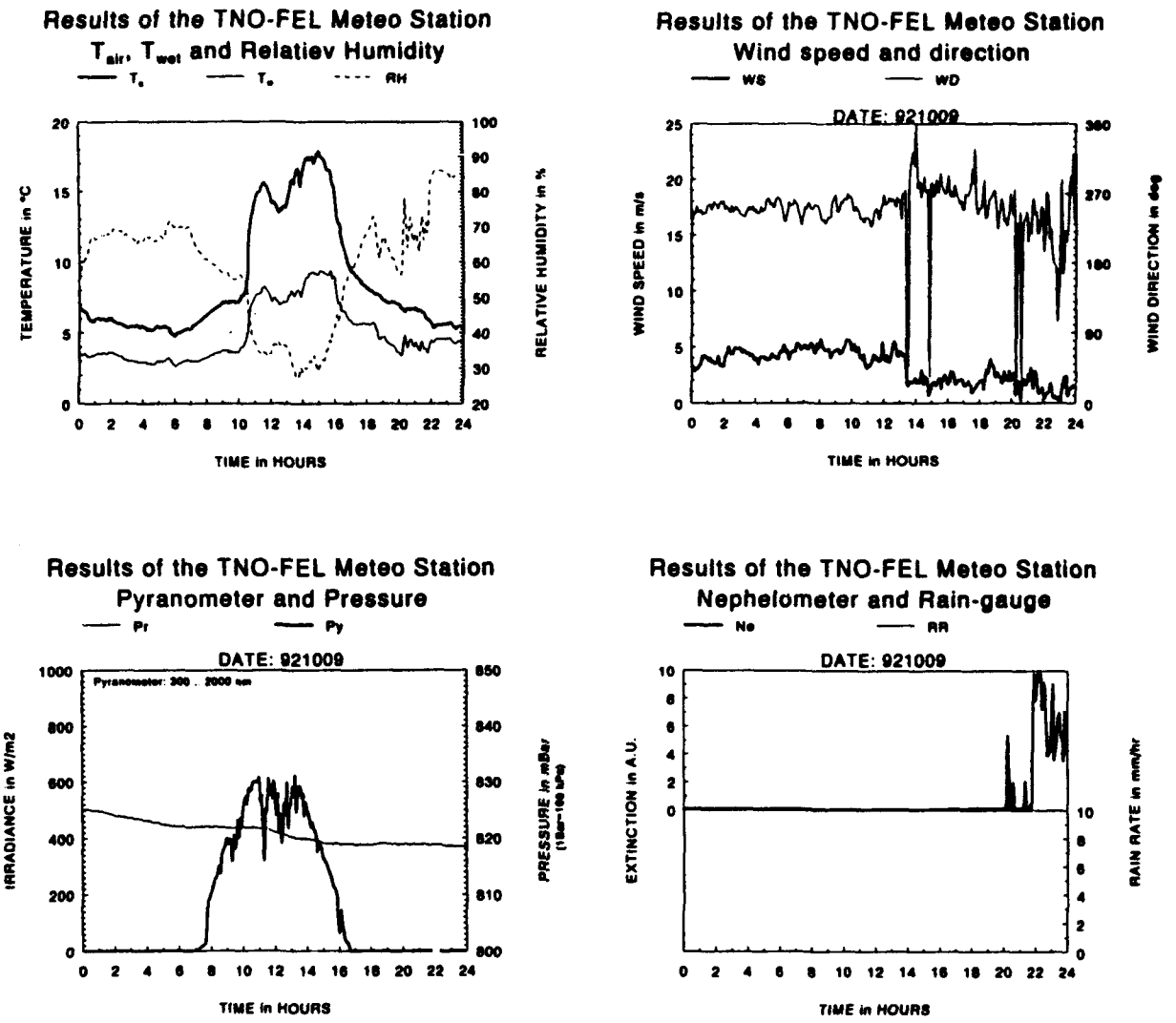


Figure 5.4: Data from the TNO meteo station at the mountain on 9 October 1992 showing dry and wet bulb temperatures, relative humidity (a), wind speed and wind direction (b), pressure and sun irradiation (c) and data from the nephelometer and rain gauge (d).

Regarding the pyranometer recording, it is noted that the meteo in the valley is often different from that at the top. For instance, in the morning of 9 October, the valley was covered with low lying clouds and filled with fog. After about 10:00 a.m., the clouds in the valley completely burned-off within a few minutes. See also Bissonnette, 1992b.

Note: The hygrophyl hygrometer is sensitive to heating by the sun. As a result, the day-time temperatures are probably too high and the calculated relative humidity is unreliable. Therefore, the use of the data from this instrument during sunshine is not recommended. In a later stage of the experiment, the sensor was shielded with polystyrene foam.

## 5.3 Turbulent fluctuations of wind speed and humidity; active periods and examples

A Gill ultra-sonic anemometer (Sonic) and an Ophir IR-2000 hygrometer were used on the 5 m high mast (see Figure 5.3) to measure the wind vector in three dimensions, the temperature (from the speed of sound) and the relative humidity at a repetition rate of 20 Hz. The data generated by these sensors can be used as additional meteo information, such as turbulence intensity, but also for calculating local turbulent fluxes (heat momentum and moisture). The turbulent intensity can be related to optical turbulence via the structure parameter $C_n^2$ which can be determined from the turbulence spectra.

All the raw data from these instruments, were stored on optical disk (WORM; capacity 800 MBy) in 6-minutes data blocks, for calculating turbulence spectra, cross-correlations and mean quantities. The dead time between the data blocks, which was required for storage, was only a few seconds. An overview of the active periods of both instruments is presented in Table 5.2. In general, the Ophir and the Sonic both operated 24 hours per day during the whole experiment, except for some short periods which were required for copying of the data and for maintenance of the Ophir.

Table 5.2: Overview of the active times of the ultra-sonic anemometer and the IR-hygrometer near Gredinger Haus.

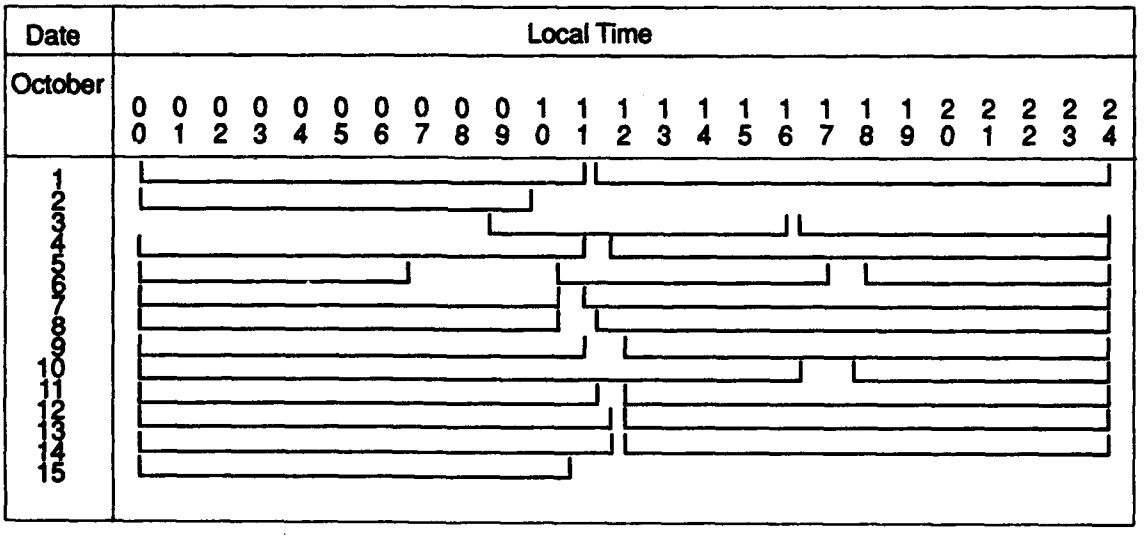


Notes:

1. The time required to copy the data from the computers' hard disk to the optical disk was about 40 minutes.
2. The amount of data generated by the Sonic and the Ophir was about 35 MBy per day.

3. In the weekend from 3 to 5 October, the instruments were not active.
4. Due to a power failure on 7 October at 06:40 hours, no data was measured during part of the morning.

Some examples of the Sonic and Ophir data

Temperatures measured by the Sonic

The ultra-sonic 3D-windsensor measures the wind speed and the speed of sound at a repetition rate of 20 Hz. Six-minutes averages and standard deviations of temperature were derived from the speed of sound. The results for 9 October 1992 are presented in Figure 5.5. Note that the temperature fluctuations vary from less than 0.2°C during darkness to a maximum of 1°C at noon. Apparently the large fluctuations in the afternoon are caused by thermal effects due to solar heating. Differences between the hygrophyl and the Sonic might be caused by difference in height, the sensitivity of the hygrophyl to the surroundings and (unknown) systematic uncertainties. At the moment, we have not compared the sonic with the other temperature sensors.

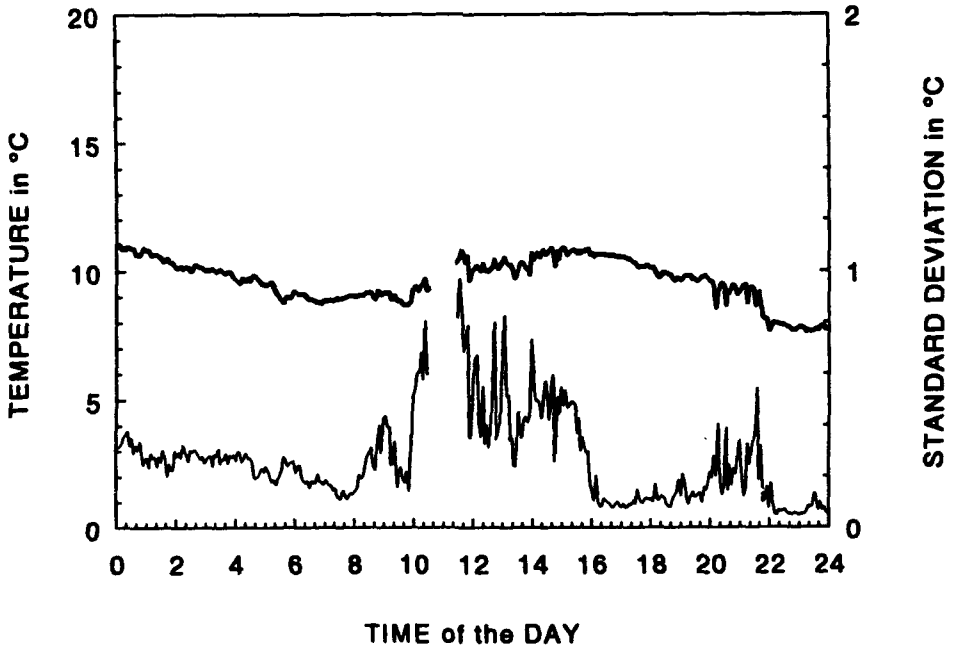


Figure 5.5: Air temperature (lhs axis, thick line) and standard deviation (rhs axis) on 9 October 1992, averaged over 6-minutes intervals, derived from the data of the ultra-sonic anemometer on the 5 m high meteo-mast near 'Gredinger Haus'.

Wind speed and direction

The horizontal and the vertical wind speed and their standard deviations, measured with the sonic anemometer on 9 October 1992, are presented in Figure 5.6. Note the excellent agreement with the results of the cup anemometer (Figure 5.4b). Note also that the standard deviation of the wind speed during the day (see the pyranometer data in Figure 5.4.c) is about a factor 2 larger than during the night.

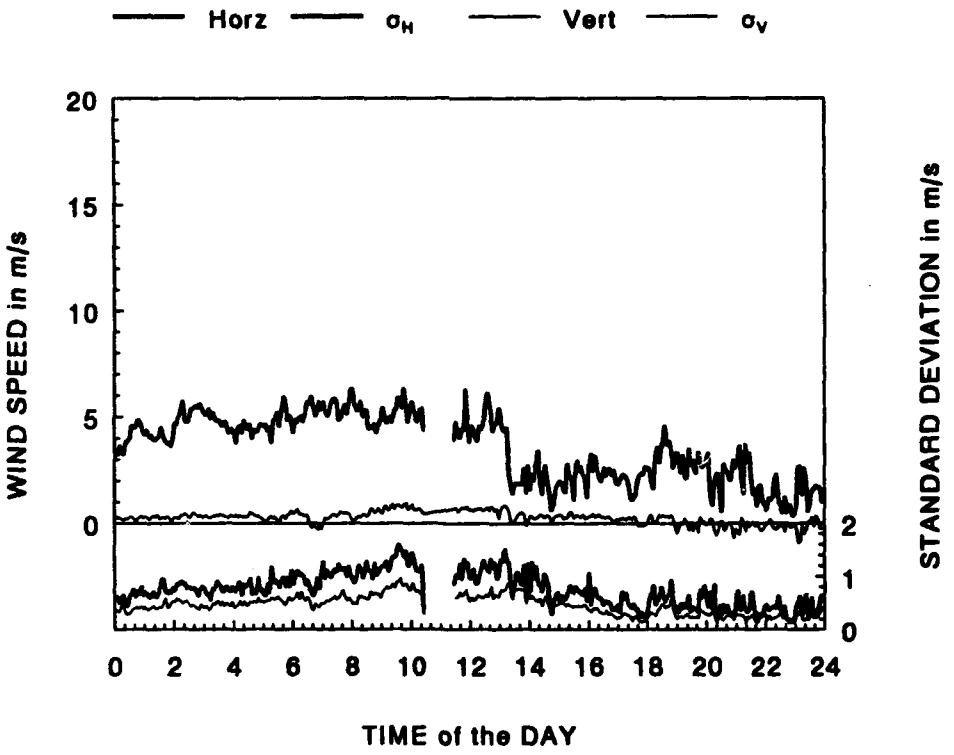


Figure 5.6: Averaged horizontal and vertical wind speed and standard deviations on 9 October 1992 near 'Gredinger Haus', as measured with the ultra-sonic anemometer.

The averaged horizontal and vertical wind direction are presented in Figure 5.7. Note the excellent agreement between the horizontal wind direction and the results of the wind vane (Figure 5.4b).

Note that there is a positive vertical wind component which might be caused by the ridge of the mountain.

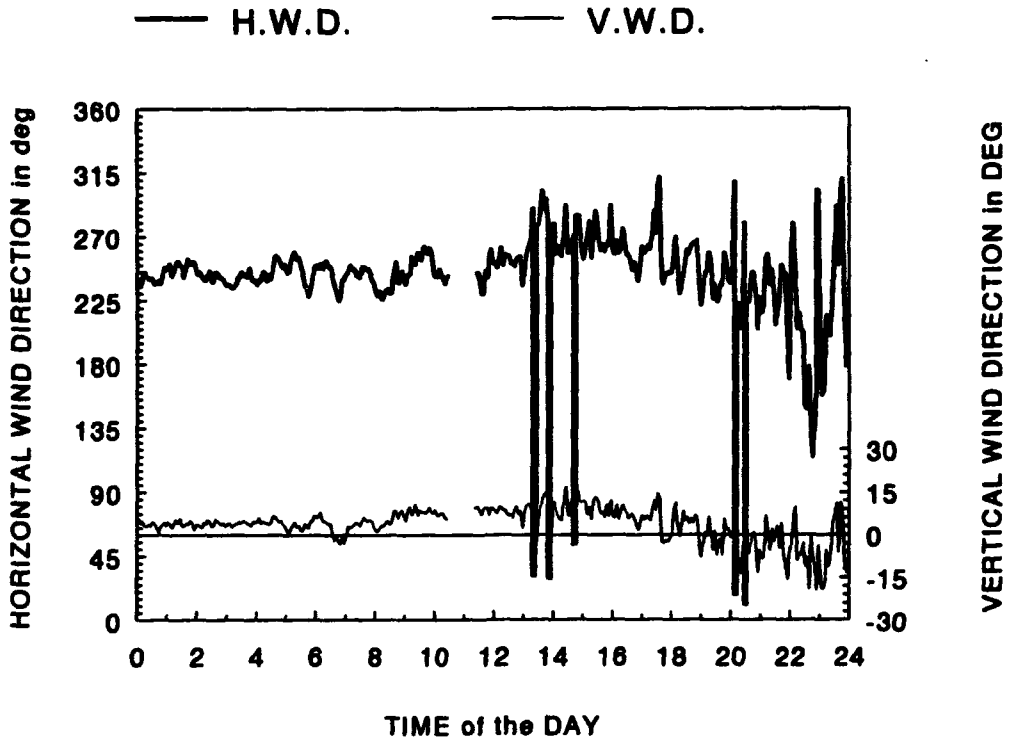


Figure 5.7: Horizontal and vertical wind direction as measured with the ultra-sonic anemometer on 9 October 1992.

Humidity

The operation of the Ophir IR-hygrometer is such that it provides 20 Hz raw data, from which the (absolute) humidity is calculated by the user. In these calculations, values are used from independent measurements of the air temperature and the internal temperature of the Ophir which are measured every 6 minutes. The internal processor of the instrument provides also the absolute and relative humidity. The externally calculated, 6-minutes averaged, values for the absolute humidity and the standard deviation for 9 October 1992, are presented in Figure 5.8. The standard deviations are about 0.2 g/kg with maximum values around 16:00 hours and after 20:00 hours.

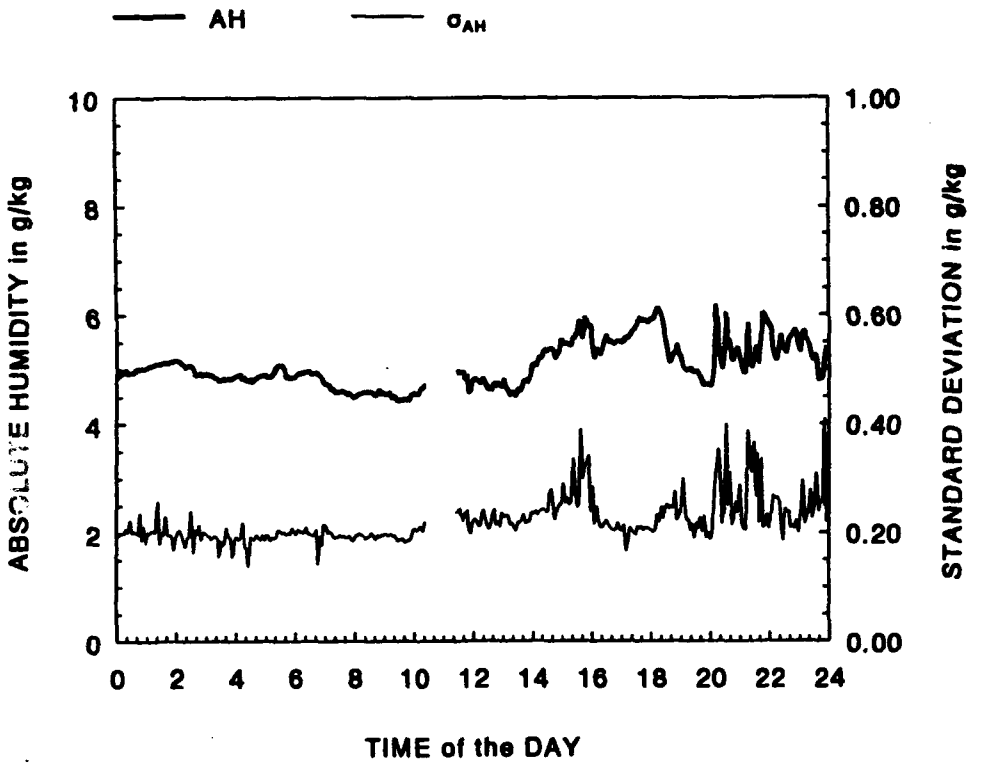


Figure 5.8: Mean and standard deviation of the absolute humidity as measured with the IR-hygrometer on the meteo mast on 9 October 1992 near 'Gredinger Haus'.

Note: To verify the calculated averaged humidity over the 6-minutes intervals, they were compared with the internally calculated humidity as shown in Figure 5.9. The figure shows that there is an offset of about 1 g/kg. This is caused by the internal calculations which use the nearest, dip switch selectable, altitude of 1830 m while the actual height is 1750 m. The two curves of the absolute humidity (indicated by AB), measured at the beginning and at the end of each 6-minute period correlate very well. This is the same for the relative humidity, indicated by RH.

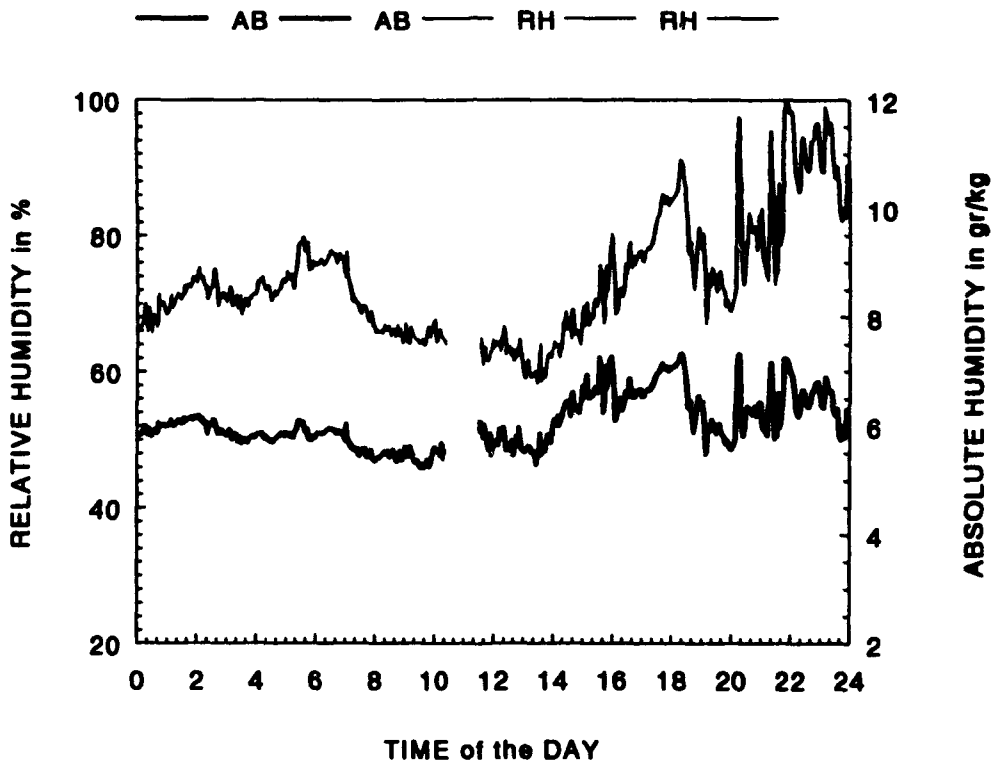


Figure 5.9: Relative and absolute humidity as provided by internal processor of the Ophir at the beginning and at the end of each 6-minutes period. Date: 9 October 1992.

Note that parts of the shape of the RH-curve (not the actual values) are comparable with the results provided by the hygrophyl shown in Figure 5.4a, dashed line.

Temperatures measured with the Ophir

The Ophir IR-humidity sensor provides also the air and the dewpoint temperature at the beginning and at the end of each 6-minute cycle. These temperatures are presented in Figure 5.10.

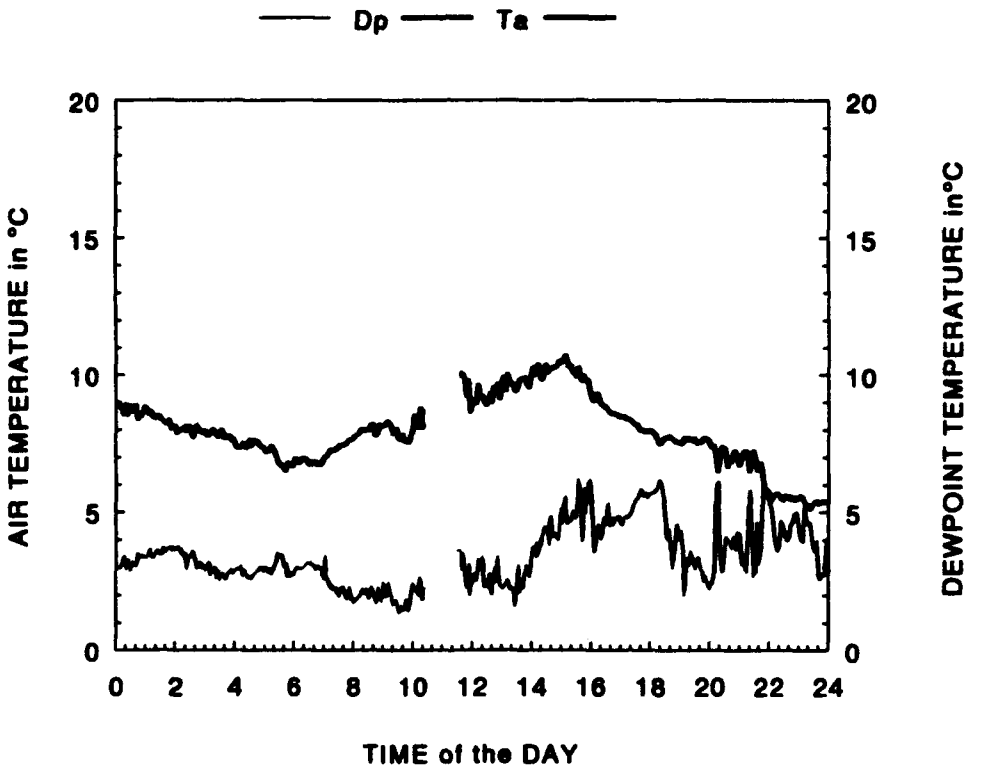


Figure 5.10: Dew point and air temperature as measured with the IR hygrometer on 9 October 1992 on the meteo mast near Gredinger Haus.

Note that during night time, there is an offset of about -2 degrees with respect to the temperature provided by the Sonic. Furthermore, the temperatures provided by the Ophir during the day are higher than from the Sonic and the variations show a slight correlation with the variations of the data from the pyranometer. Therefore, it seems that the Ophir is also sensitive to solar heating.

Spectra of wind, temperature and humidity

Turbulent spectra of air-flow components, temperature and humidity can be calculated from the 20 Hz data obtained from the ultra-sonic anemometer and the IR humidity sensor. These spectra

provide basic information to determine the inertial subrange of the eddies and the structure constants. This might be important e.g. for comparison with data from the ATMOS turbulence sensor or with the IR-images. Furthermore, the temperature and humidity time series can be used to calculate the local variation in the refractive index and thus its structure constant (using Taylor's hypothesis). Some of the spectra, calculated from the 9 October data at 07:00, 11:30 and 17:00 o'clock, are presented in Figure 5.11a...d.

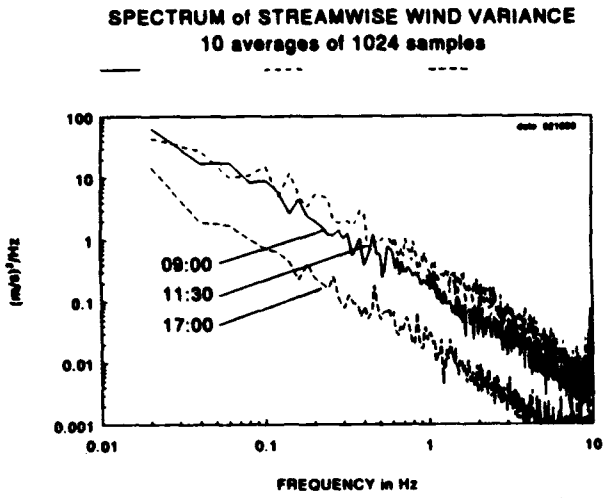


Figure 5.11a: Variance spectrum of the streamwise (horizontal) wind speed.

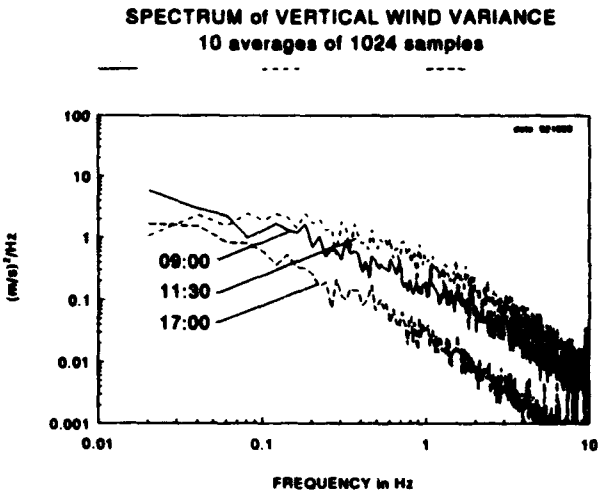


Figure 5.11b: Variance spectrum of the vertical wind speed.

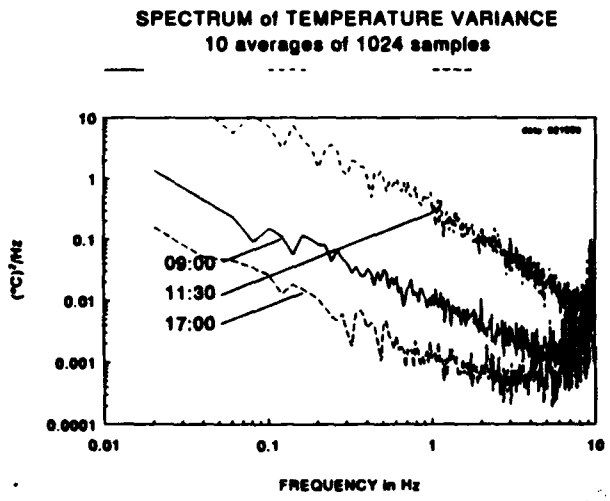


Figure 5.11c: Variance spectrum of the temperature.

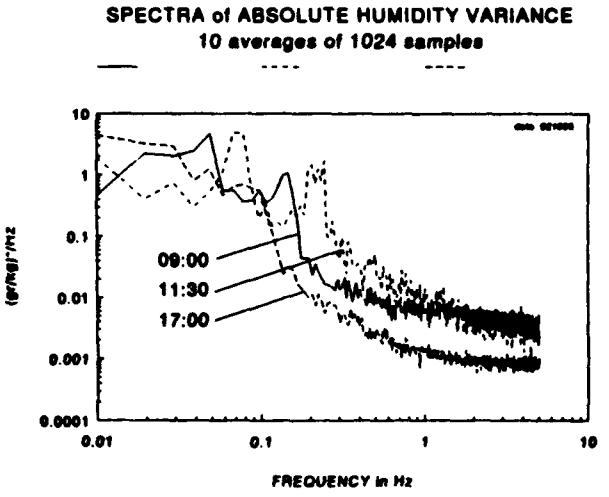


Figure 5.11d: Variance spectrum of the absolute humidity.

The streamwise (horizontal) and the vertical wind variance spectra show the Kolmogorov decay (power -5/3) from which the inertial subranges can be determined. The temperature variances also show this behaviour. (High frequency spikes in some of the spectra might be caused by the eigen frequencies of the meteo mast.) The humidity variance spectra do not show the well known Kolmogorov behaviour. We cannot explain whether this is a true atmospheric behaviour or an instrument deficiency.

Correlations

The variations in wind speed, temperature and humidity time series, can be cross-correlated to calculate turbulent fluxes e.g. the turbulent momentum, heat and humidity flux. An example of such a correlation calculation between the streamwise wind speed and the temperature, <s.t>, and between the vertical wind speed and the temperature, <w.t>, (respectively the horizontal and vertical kinematic turbulent heat flux) are presented in Figure 5.12. (The results are probably influenced by the mountain.)

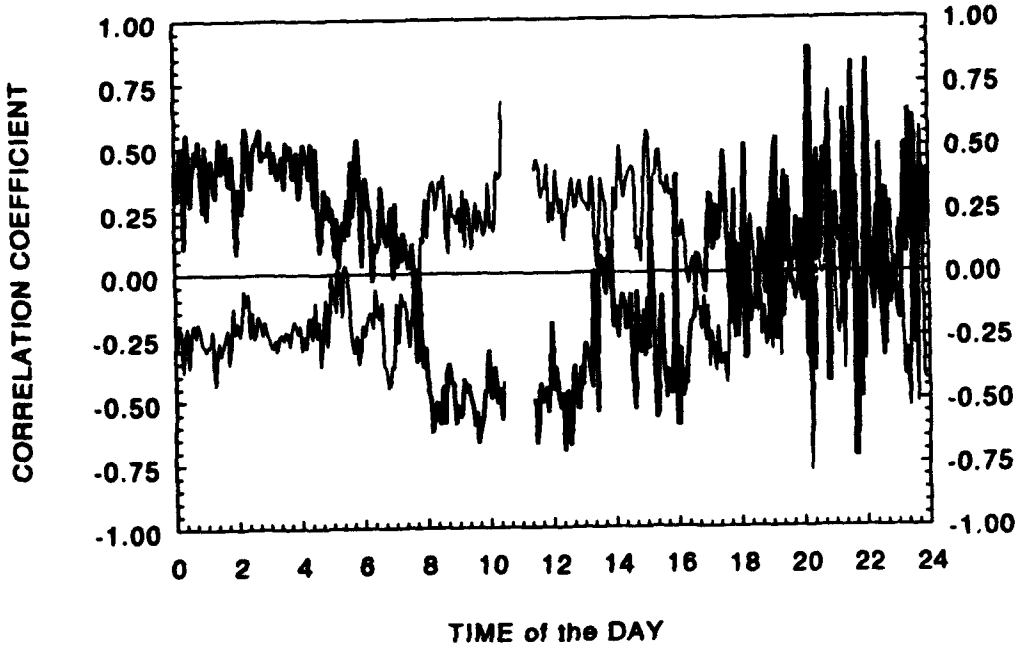


Figure 5.12: Correlation between the streamwise wind speed and the temperature, <s.t> (solid line), and the vertical wind speed and the temperature; <w.t> (thin line). (Data from utra-sonic anemometer, 9 October 1992).

Figure 5.12 shows that the correlation between the horizontal (streamwise) wind speed and the temperature is positive during the night and morning, but negative short after sunrise and during the day. The opposite is true for the correlation between the vertical wind and the temperature. This might be caused by a downward turbulent heat transport during the night and an upward turbulent heat transport during the day. After sunset the correlation between the wind and the temperature varies strongly.

## 5.4 Aerosol probes; active periods

Aerosol measurements were performed with the following equipment from Particle Measuring Systems, Boulder, Co, USA:

- ASAS 300A
- CSAS 100 HV

The probes were not operated unattended during the experiment because aspirated water would damage the instrument in cases of rain and heavy fog.

Table 5.3: Overview of the active times of the TNO-aerosol probed near Gredinger Haus.

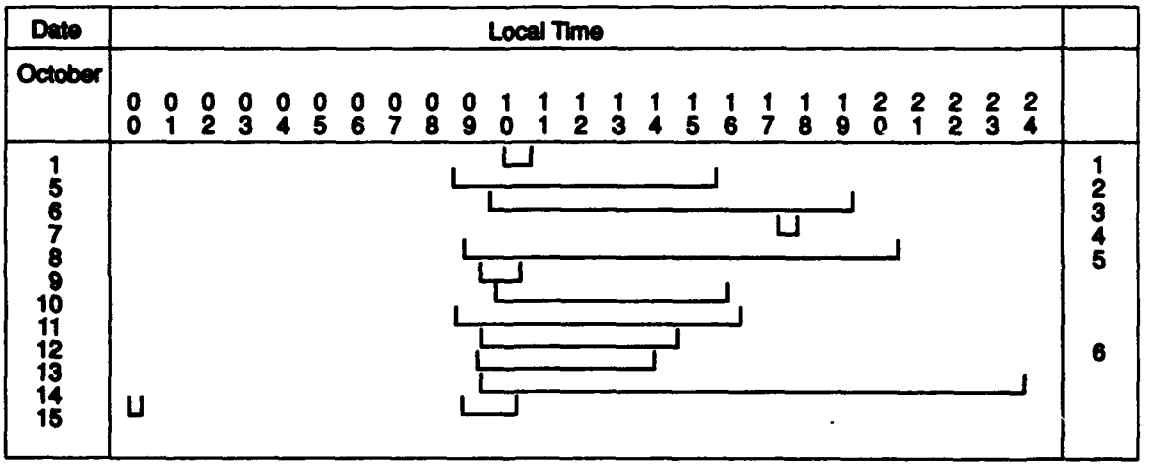


Remarks:

1. visibility about 36 km
2. defect ASAS 300 A-probe
3. clear day
4. heavy clouds
5. dissolving clouds
6. visibility smaller than 100 m

# 6 CONCLUSIONS

An overview has been presented of the TNO instrumentation and experiments during NATO experiment VAST92, illustrated with some typical examples. A number of data sets have been processed to demonstrate the possibilities of the different instruments for instance for the calculation of the turbulent fluctuations of temperature, wind speed and humidity.

The altitude of the cable car was determined with a pressure sensor. An empirical relation has been derived to convert pressure to altitude which is within 3% of the theory.

This report will be used as a guide-line for processing the TNO data in conjunction with data from other participants and will inform the other participants on the availability of the TNO data. Interpretation of the results is postponed to later reports.

ACKNOWLEDGMENT

VAST 92 was a perfectly organized and directed trial with clear discussions and new contacts between the different participants. We appreciate the cooperation and the contacts with the other participants. The hospitality of the proving ground and the cooperation with the proving ground personnel was excellent.

## REFERENCES

BISSONNETTE, L.R. 'Final workplan for the vertical atmospheric structure trial 1992 (VAST 92) organized by NATO AC/243 Panel 4/RSG.8 on Atmospheric propagation effects on electro-optical systems'
Defence Research Establishment Valcartier, Canada, 1 June 1992a

BISSONNETTE, L.R., 'Quick look data report'
NATO AC/243 Panel 4/RSG.8, 16 November 1992b

KUNZ, G.J. 'A high repetition rate LIDAR'
TNO-Physics and Electronics Laboratory
FEL-90-A352, April 1991

| | | |
|---|---|---|
| A.N. de Jong | G.J. Kunz | M.M. Moerman |
| (group leader) | (author) | (author) |

## RELATION BETWEEN PRESSURE AND ALTITUDE

(Equations (A.1)-(A.10) provided by Dr. J. Martin, ASL USA)

The simplest method for height as a function of pressure and temperature for the test at Oberjettenberg is the following:

$$Z = \frac{T_0}{\alpha} \cdot \left[ 1 - \left\{ \left( 1 - \alpha \cdot \frac{Z_0}{T_0} \right) \cdot \left( \frac{P}{P_0} \right) \cdot \alpha \cdot R \right\} \right] \qquad \text{(A.1)}$$

where:

$\alpha$ = temperature lapse rate, ≈ 0.0065 K/m
$P$ = pressure at height Z in mBar
$P_0$ = pressure at reference height in mBar
$R$ = gas constant, 29.2745 m/K
$T_0$ = temperature at reference height $Z_0$ in K
$Z$ = height in m
$Z_0$ = reference height, 650 m (valley station)

The derivation of equation (A.1) is based on the following assumptions:

a) the atmosphere is an ideal gas

$$P = s \cdot g \cdot R \cdot T \qquad \text{(A.2)}$$

where:

$g$ = acceleration of gravity, 9.80665 m/s$^2$
$s$ =
$T$ = temperature in K

b) the temperature lapse rate is constant

$$T = T_0 - \alpha \cdot Z \qquad \text{(A.3)}$$

The mentioned lapse rate for temperature, $\alpha$, may not be indicative for the situation at Oberjettenberg but can be calculated from:

$$\alpha = \frac{1}{R} \cdot \frac{\ln\left(\frac{T}{T_0}\right)}{\ln\left(\frac{P}{P_0}\right)} \qquad (A.4)$$

Derivation of equation (A.1)

Starting with Newtons fundamental law of motion and using gravity as the acceleration force:

$$F = m \cdot g \qquad (A.5)$$

Now, pressure is a force per unit area A, or:

$$P = \frac{F}{A} \qquad (A.6)$$

and the mass of the atmosphere above the unit area is:

$$m = s \cdot A \cdot z \qquad (A.7)$$

where:

z = total height of the column of air above the point in question.

Substitution of equation (A.5) and (A.7) in (A.6) provides:

$$P = s \cdot g \cdot z \qquad (A.8)$$

The differential form of this equation is:

$$dP = -s \cdot g \cdot dZ \qquad (Z = \text{constant} - z) \qquad (A.9)$$

Substitution for s, using the ideal gas law (A.2) we find:

$$\frac{dP}{P} = \frac{-1}{R \cdot T} \cdot dZ \qquad (A.10)$$

Substitution of equation (A.3) in (A.10) and integrating from some reference height $Z_0$ with pressure $P_0$, provides equation (A.1).

To study the influence of temperature and temperature lapse rate on the relation between pressure and height, equation (A.1) has been plotted in Figure A1 for different reference pressures, different reference temperatures and different lapse rates.

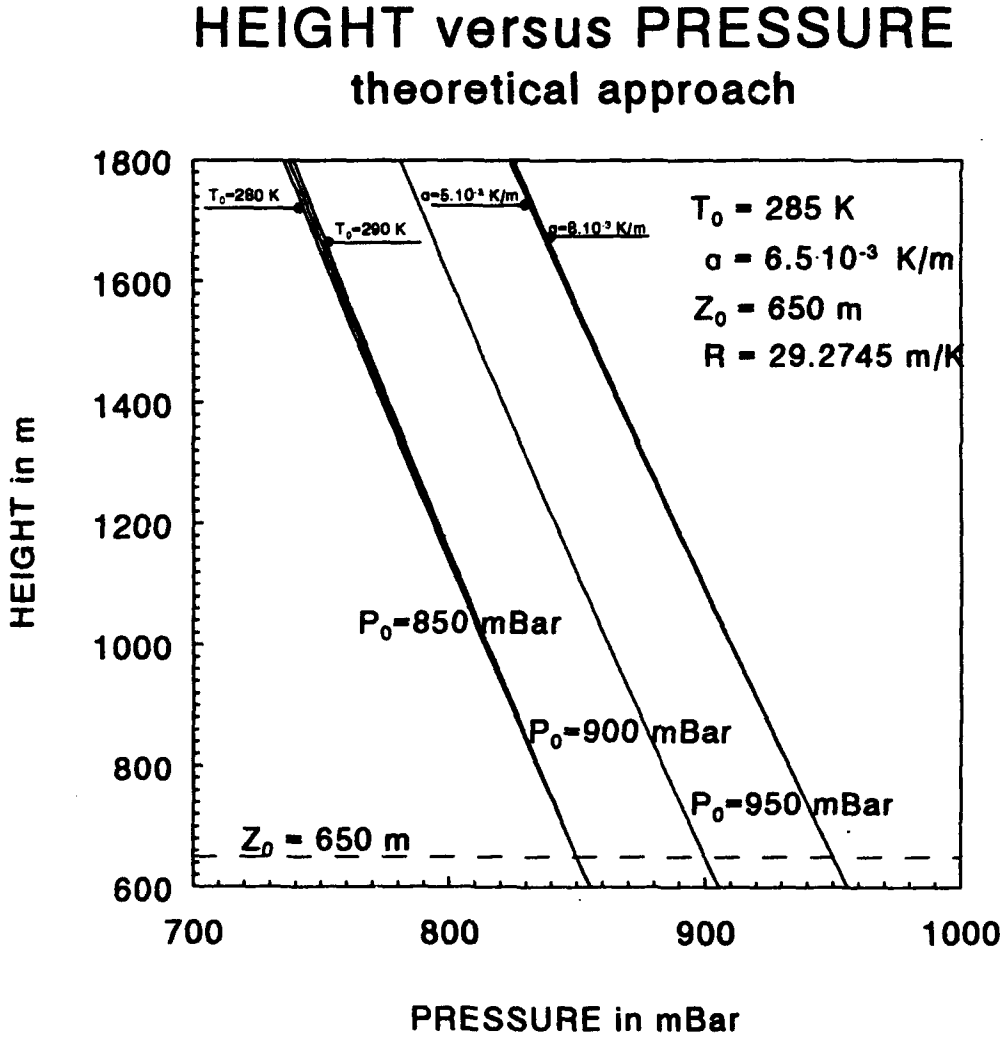


Figure A1: Relation between pressure and height for three reference pressures for the VAST 92 situation. The influence of temperature and temperature lapse rate is indicated in respectively the 850 and 950 mBar curves.

The results of Figure A1 indicate that (in the range and pressure interval during VAST 92) the relation between height and pressure is almost linear. The slope depends slightly on temperature and reference pressure. The temperature lapse rate, $\alpha$, has little influence on the curve.

The slope of the curves in Figure A1 has been studied in more detail by differentiating equation (A.1) with respect to pressure. This yields the following result:

$$\frac{dZ}{dP} = \frac{-R \cdot T_0}{P_0}\left(1-\alpha \cdot \frac{Z_0}{T_0}\right) \cdot \left(\frac{P}{P_0}\right)^{(-1+\alpha \cdot R)} \qquad \text{(A.11)}$$

This differential quotient is plotted in Figure A2 as a function of the pressure P.

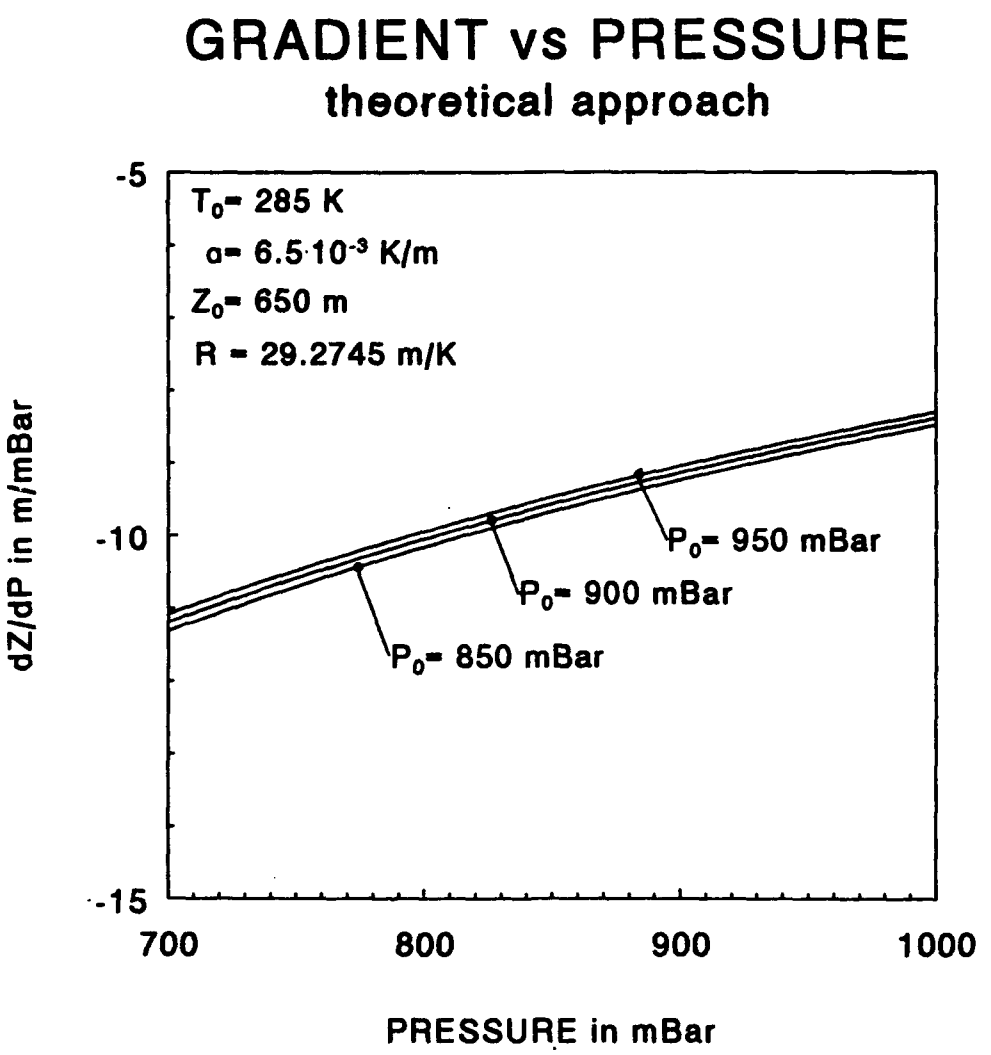


Figure A2: Dependence of the differential quotient dZ/dP as a function of the pressure for three reference pressures.

During VAST 92, the reference pressure at the reference height (valley cable car station at 650 m height) varied between about 920 and about 940 mBar. At the mountain station, the pressure varied between about 820 and about 840 mBar. As a result, the averaged differential quotient dZ/dP over this interval is about 9.2 m/mBar.

Experimentally, an averaged value of 9.5 m/mBar was found. The difference between theory and experiment of about 3% might be caused by the non adiabatic lapse rate of temperature, the uncertainty of the absolute calibration of the pressure sensor and/or the strain of the cable.

# REPORT DOCUMENTATION PAGE (MOD-NL)

**1. DEFENSE REPORT NUMBER (MOD-NL)**
TD93-0480

**2. RECIPIENT'S ACCESSION NUMBER**

**3. PERFORMING ORGANIZATION REPORT NUMBER**
FEL-93-A039

**4. PROJECT/TASK/WORK UNIT NO.**
22392

**5. CONTRACT NUMBER**
A90K703

**6. REPORT DATE**
AUGUST 1993

**7. NUMBER OF PAGES**
42 (INCL. 1 APPENDIX, EXCL. RDP + DISTRIBUTION LIST)

**8. NUMBER OF REFERENCES**
3

**9. TYPE OF REPORT AND DATES COVERED**

**10. TITLE AND SUBTITLE**
AN OVERVIEW OF THE TNO CONTRIBUTION TO VAST 92

**11. AUTHOR(S)**
G.J. KUNZ
M.M. MOERMAN

**12. PERFORMING ORGANIZATION NAME(S) AND ADDRESS(ES)**
TNO PHYSICS AND ELECTRONICS LABORATORY, P.O. BOX 96864, 2509 JG THE HAGUE
OUDE WAALSDORPERWEG 63, THE HAGUE, THE NETHERLANDS

**13. SPONSORING/MONITORING AGENCY NAME(S)**
ROYAL NETHERLANDS NAVY

**14. SUPPLEMENTARY NOTES**
THE CLASSIFICATION DESIGNATION ONGERUBRICEERD IS EQUIVALENT TO UNCLASSIFIED.

**15. ABSTRACT (MAXIMUM 200 WORDS, 1044 POSITIONS)**
THE 'VERTICAL ATMOSPHERIC STRUCTURE TRIAL' (VAST92) TOOK PLACE FROM 28 SEPTEMBER TO 16 OCTOBER 1992 AT THE WEHR TECHNISCHE DIENSTSTELLE (WTD 52), OBERJETTENBERG, GERMANY, IN THE FRAMEWORK OF NATO WORKING GROUP AC/243 (PANEL 4/RSG.8) ON ATMOSPHERIC PROPAGATION EFFECTS ON ELECTRO-OPTICAL SYSTEMS. THE EXPERIMENT WAS DESIGNED TO QUANTIFY THE INFLUENCE OF THE ATMOSPHERIC VERTICAL STRUCTURE VARIATIONS ON INFRARED PROPAGATION AND IMAGING AND ON LIDAR MEANS OF REMOTELY SENSING THE VARIATIONS. THE TNO-PHYSICS AND ELECTRONICS LABORATORY PARTICIPATED WITH A LIDAR SYSTEM, METEO AND AEROSOL EQUIPMENT. THE LIDAR WAS STATIONED IN THE VALLEY. AN ALTIMETER AND METEO-EQUIPMENT WERE MOUNTED ON THE CABLE CAR. AEROSOL SPECTROMETERS AND METEOROLOGICAL EQUIPMENT WERE USED, INCLUDING A SONIC ANEMOMETER AND A FAST HYGROMETER TO MEASURE TURBULENCE ON THE MOUNTAIN. A LARGE PART OF THE DATA FROM THESE INSTRUMENTS IS OF CRUCIAL IMPORTANCE FOR THE EVALUATION AND INTERPRETATION OF THE DATA OBTAINED BY THE OTHER PARTICIPANTS.

IN THIS REPORT, WE PRESENT AN OVERVIEW OF THE TNO INSTRUMENTATION AND EXPERIMENTS. A NUMBER OF DATA SETS HAVE BEEN PROCESSED TO DEMONSTRATE THE POSSIBILITIES OF THE DIFFERENT INSTRUMENTS. INTERPRETATION OF THE RESULTS IS POSTPONED TO LATER REPORTS. THIS REPORT IS ALSO A GUIDE-LINE FOR PROCESSING THE TNO DATA IN CONJUNCTION WITH DATA FROM OTHER PARTICIPANTS.

**16. DESCRIPTORS**
METEOROLOGICAL EXPEDITIONS
ATMOSPHERIC PROPAGATION
LASER RADAR (LIDAR)
ATMOSPHERIC STRUCTURE

**IDENTIFIERS**
OPTICAL PROPERTIES
VERTICAL PROFILES

**17a. SECURITY CLASSIFICATION (OF REPORT)**
ONGERUBRICEERD

**17b. SECURITY CLASSIFICATION (OF PAGE)**
ONGERUBRICEERD

**17c. SECURITY CLASSIFICATION (OF ABSTRACT)**
ONGERUBRICEERD

**18. DISTRIBUTION/AVAILABILITY STATEMENT**
UNLIMITED

**17d. SECURITY CLASSIFICATION (OF TITLES)**
ONGERUBRICEERD